Thesis Title

A subtitle of your thesis

Author name

Thesis submitted for the degree of
Master in Master's Program Name <change at main.tex>
60 credits

Department Name <change at main.tex>
Faculty name <change in duoforside.tex>

UNIVERSITY OF OSLO

Spring 2022

Thesis Title

A subtitle of your thesis

Author name

Thesis Title

http://www.duo.uio.no/

Printed: Reprosentralen, University of Oslo

Abstract

Contents

1 Introduction **1**

I Theory **3**

2 High-Entropy alloys **4**
2.1 Fundamentals 4
2.2 Core effects and properties 7

3 Modeling of random alloys **9**
3.1 The Special Quasi-random Structure model 9
3.1.1 Mathematical description 10
3.1.2 Applications to high-entropy alloys 12

4 Density Functional Theory **16**
4.1 Review of Quantum Mechanics 17
4.1.1 The Shrodinger equation 17
4.1.2 Approximations to the many-body Shrodinger equation 18
4.2 Kohn-Sham density functional theory 20
4.2.1 Density functional theory 20
4.2.2 The Kohn-Sham Equation 21
4.3 Limitations of DFT - Insert refs 22

II Methodology and Implementation **24**

6 Practical application of DFT **23**
6.1 The Exchange-Correlation functional 23
6.2 Fundamental aspects of practical DFT calculations 24
6.3 Self-consistent field calculation 26

7 Computational details **28**
7.1 Vienna Ab initio Simulation Package 28
7.2 Generation of SQS 30
7.3 Figures 31
7.3.1 Density of states 31
7.3.2 Probability distribution functions 31

7.3.3 Charge density 31
7.4 Band gap 31
7.5 Utility scripts 31

III Results and Discussion **33**

8 The results of (CrFeMnNi)Si_2 in the $\beta-FeSi_2$ structure **33**
8.1 Eqvimolar SQSs 33
8.1.1 Introduction 33
8.1.2 The band gap 34
8.1.3 Local and Projected density of states 36
8.1.4 Meta-GGA and hybrid functional 40
8.1.5 Probability distribution functions and charge density 44
8.2 Permutations of the $Cr_4Fe_4Mn_4Ni_4Si_{32}$ high-entropy silicide 46

9 Changing the elements **52**

10 Overview and Relevance **57**
10.1 $Cr_4Fe_4Mn_4Ni_4Si_{32}$ in different crystal structures 57
10.2 Overview 59

IV Conclusion **60**

A Density of states **56**

B PDFs **57**

C Charge density **58**

List of Figures

2.1 Formation of HEA based on δ and N. Figures adopted from [15] . . . 6
2.2 A schematic illustration of lattice distortion in high-entropy alloys. Figure from [3] . . . 8

3.1 PDFs of (a) 20 and (b) 250 atom SQS models of CrFeMnNi [1] 13
3.2 Density of states with SQS and MC/MD of FCC CoCrFeNi, figure from [1] . . . 14
3.3 Probability distribution functions with SQS and MC/MD of HCP CoOsReRu [1] . . . 14

4.1 Number of DFT studies per year from 1980 to 2021 [**dimensions**]. . . . 16

6.1 Self consistent iteration of a DFT calculation. Figure adopted from lecture notes fys-mena4111 **cite** . . . 27

7.1 48 atom SQS based on eqvimolar distribution of Cr, Fe, Mn and Ni in and $FeSi_2$ cell. . . . 32

8.1 Density of states SQS D CFMN (fesi2) from PBE calculation . 35
8.2 Density of states SQS B CFMN (fesi2) from PBE calculation . 36
8.3 Local density of states of Si (SQS D) . . . 37
8.4 Local density of states of TMs (SQS D), (a) Cr, (b) Mn, (c) Fe, (d) Ni . . . 37
8.5 Projected density of states SQS D CFMN (fesi2) from PBE calculation . . . 38
8.6 Projected density of states of SQS D and B around E_F 38
8.7 Density of states of SQS C with 2501 points vs 20000 points in the density of states. . . . 39
8.8 Density of states of SQS E illustrating the different band gap from calculations with (a) PBE and (b) SCAN functional . . . 41
8.9 Total density of states of SQS (a) B and (b) E from calculations with HSE06 . . . 42
8.10 Probability distribution function of SQS D (top) and B (bottom) 45
8.11 Charge density of SQS D and B from PBE calculations. Illustrated by VESTA . . . 46

8.12 Projected density of states of (a) $Cr_3Fe_3Mn_7Ni_3Si_{32}$ (SQS B), (b) $Cr_5Fe_5Mn_3Ni_3Si_{32}$ (SQS C), (c) $Cr_5Fe_3Mn_5Ni_3Si_{32}$ (SQS A), (d) $Cr_3Fe_5Mn_5Ni_3Si_{32}$ (SQS D) 49
8.13 Density of states around E_F of SQS D and E $Cr_5Fe_5Mn_3Ni_3Si_{32}$ 50
8.14 Projected density of states of $Cr_3Fe_3Mn_3Ni_7Si_{32}$ around E_F . 50
8.15 Probability distribution functions to $Cr_3Fe_5Mn_5Ni_3Si_{32}$ SQS D, **Maybe make larger** 51

9.1 Projected density of states of $Cr_4Fe_4Co_4Ni_4Si_{32}$ 54

List of Tables

8.1 Total energy per atom, final magnetic moment, band gap (GGA) and formation enthalpy of $Cr_4Fe_4Mn_4Ni_4Si_{32}$ SQSs based on $FeSi_2$ 34
8.2 Band gap transition of CFMN (fesi2) SQSs with PBE functional 35
8.3 Band gap (eV) with PBE in spin up and spin down channels of CFMN (fesi2) SQSs 36
8.4 Band gap of CFMN ($FeSi_2$) SQSs with GGA (PBE), meta-GGA (SCAN) and hybrid-functionals (HSE06). 40
8.5 Mean and stadard deviation of the total energy and magnetic moment per atom, plus enthalpy of formation of the listed mean energies ($FeSi_2$). 47
8.6 Total and spin dependent band gap of 4 permutations of CFMN (fesi2) with PBE GGA calculation. The structures that are excluded from this list either failed in calculations, or does not show any band gap.< 48

9.1 Summary of the total energy, enthalpy of formation and magnetization of several composistionally different SQS high-entropy alloys based on the $\beta-$ $FeSi_2$ unit cell. 52

Preface

Chapter 1

Introduction

some introduction on the importance of discovering new materials and alloying.
Need something on thermoelectricity related to both the band gap and high-entropy alloys.

High-entropy alloys is a novel class of materials based on alloying multiple components, as opposed to the more traditional binary alloys. This results in an unprecedented opportunity for discovery of new materials with a superior degree of tuning for specific properties and applications. Recent research on high-entropy alloys have resulted in materials with exceedingly strong mechanical properties such as strength, corrosion and temperature resistance, etc **find references**. Meanwhile, the functional properties of high-entropy alloys is vastly unexplored. In this study, we attempt to broaden the knowledge of this field, the precise formulation of this thesis would be an exploration on the possibilities of semiconducting high-entropy alloys.

A key motivation of this thesis is the ability to perform such a broad study of complex materials in light of the advances in material informatics and computational methods. In this project, we will employ Ab initio methods backed by density functional theory on top-of the line supercomputers and software. 20 years ago, at the breaking point of these methods, this study would have been significantly narrower and less detailed firstly, but secondly would have totaled ... amount of CPU hours to complete (**Calculate this number**). In the addition to the development in computational power, is also the progress of modeling materials, specifically we will apply a method called Special Quasi-random Structures (SQS) to model high-entropy alloys or generally computationally complex structures. Together with the open landscape of high-entropy alloys described above, these factors produce a relevant study in the direction of applying modern computational methods to progress the research of a novel material class and point to promising directions for future research.

In specifics, this thesis revolve around the electrical properties of high-entropy alloys, mainly the band gap as this is the key indicator for a semiconducting material and it's applicability. Semiconductors are the building blocks in many different applications in today's world, ranging

from optical and electrical devices, to renewable energy sources such as solar and thermoelectricity. Given the economic and sustainable factors concerning silicon, in addition to its role in relevant applications such as microelectronics and solar power. Silicon emerges as a natural selection to build our alloys around. Furthermore, the development and research on both high entropy alloys and metal silcides have been heavily centered around 3d transition metals. Keeping in line with the economic and environmental factors, we will continue this direction by focusing on high entropy stabilized sustainable and economic 3d metal silicides **Not happy with this writing**. Throughout the study we will analyze a great number of permutations of 3d silicides, from different initial metal silicides such as $CrSi_2$, $FeSi_2$, $MnSi_{1.75}$, Fe_2Si, each with distinct properties relating to the band gap, crystal structure and metal to silicon ratio. In addition, the permutations include numerous metal distributions and elements within the 3d-group of metals. Examples are Co, Cr, Fe, Mn, and Ni.

Given a background in high-entropy alloys, one could ask if this study is truly sensible. In the later sections we will cover the details of this field, and it quickly become clear that the materials investigated in this study does not fall under the precise definition of high-entropy alloys, nor do we intend to explore the properties and factors relating to high-entropy stabilized alloys such as the configurational entropy, phase stability and finite temperature studies. However this study is motivated from the discovery of these materials and promising properties, and venture into a more hypothetical space of materials, enabled by the computational methods available to study the potential properties of such materials. On the other hand, very recent studies **Mari, and other HEA silicide study** have experimentally synthesized high-entropy disilicides, thus in some way justifying the direction of this project.

We begin this project by reviewing key concepts of solid-state physics for readers lacking a background in materials science, and an introduction to the base 3d silicides of the experimental work. Later follows a theoretic walk-through of the relevant concepts of this thesis, these topics include high-entropy alloys, special quasi-random structures, and density functional theory. Next we shine light on the implementation of DFT in this project, and other computational details required to reproduce the results in this thesis, such as the use of the Vienna Ab Initio Simulation Package (VASP) and implementation of SQS. Finally we present the results of our study, these include the band gap and electronic properties of various structures and the success and challenges of the computational methods applied throughout the study.

Part I

Theory

Chapter 2

High-Entropy alloys

To begin this project, we give a brief description of high-entropy alloys (HEA). We introduce the basics and definitions, as well some more advanced topics relating to the functional properties of HEA's. This section will be largely based on the fantastic description of HEAs in "High-Entropy Alloys - Fundamentals and Application" and the references therein, it's an excellent read. This section is particularly based on chapters 1,2,3, and 7 [12], [15], [13], [14]

2.1 Fundamentals

High-Entropy Alloys are a quickly emerging field in materials science due to the infinitely many possibilities and the unique properties. From the original discovery by Jin in 2004, as of 2015 there have been over 1000 published journal articles on high-entropy alloys. In its simplicity, a high-entropy alloy can be compared to a smoothie. By combining an assortment of fresh fruit and vegetables one can produce unique combinations of flavors and nutritional values based on both the properties of the distinct items, and their interplay in the mixture. In materials science, this exact procedure can be applied to generate a large range of materials with tunable properties depending on the intended application. In the topic of HEA's, this can be increased strength or ductility, corrosive resistance or lowered thermal conductivity, all of which have been observed in actual high-entropy alloys. Moving on from the rather banal fruit analogy, a high-entropy alloy typically falls under the two conditions.

1. The material consist of at least 5 distinct elements, where each element contribute between 5-35% of the composition
2. The total configurational entropy is greater than 1.5R, where R is the gas constant.

The latter is an especial case for high-entropy alloys. The ideal configurational entropy of random N-component solid-solution is given in eq 2.1

$$\Delta S_{\text{config}} = -R \sum_{i=1}^{N} X_i \ln X_i, \tag{2.1}$$

it's clear that ΔS_{config} increase with a higher number of constituents in the mix. For instance, the ideal configurational entropy of a binary alloy is $0.69R$, while a 5-component alloy is $1.61R$. If we neglect other factors that influence the formation of solid solutions (will be covered later), from Gibbs free energy in eq 2.2

$$\Delta G_{\text{mix}} = \Delta H_{\text{mix}} - T\Delta S_{\text{mix}}, \tag{2.2}$$

the two primary factors in formation of solid solution is the mixing enthalpy, which is the driving force to form compounds, and the mixing entropy which is the driving force to form random solid solutions. At elevated temperatures especially, the energy associated to the entropy of the system becomes comparative to the mixing enthalpy and can impact the overall equation. In summary, the overall concept of high-entropy alloys is that through alloying a greater number of elements, the gain in configurational entropy of the system prohibit the formation of intermetallic compounds in favor of a random solid solution. The random term simply relate to the various components occupying lattice positions based on probability. In fact, a narrower definition of high-entropy alloys would be structures with a single-phase disordered solid solution. The two "definitions" given previously can be considered as guidelines for the latter.

All though the mixing entropy mentioned above plays a central role in the formation, there are other factors to consider, and some that may oppose the formation of a single disordered phase. One of these is the atomic size effect which is related to the differences in atomic size, between the various elements in the alloy, this quantity is denoted δ. Y. Zhang et al. in 2008 illustrated the relationship between ΔH_{mix} and δ. When δ is very small, ie similar atomic sizes. The elements have an equal probability to occupy lattice sites to form solid solutions, but the mixing enthalpy is not negative enough to promote formation of solid solution. Increasing δ does result in greater ΔH_{mix}, but leads to a higher degree of ordering. **Include figure?**To summarize the illustration, the formation of solid solution high-entropy alloys occur in a narrow range of δ value that satisfy both the enthalpy of mixing and the disordered state. Recently, Yang and Zhang proposed the parameter Ω to evaluate the stability of high-entropy alloys. The quantity is a product of the melting temperature T_m, mixing entropy and mixing enthalpy in the following manner

$$\Omega = \frac{T_{\text{m}}\delta S_{\text{mix}}}{|\Delta H_{\text{mix}}|}. \tag{2.3}$$

They managed to obtain a qualitative condition for formation of the single disordered solid solution at $\Omega \geq 1.1$ and $\delta \leq 6.6\%$. While compounds such as intermetallics form for greater values of δ and lesser values of Ω. Similarly, replacing the atomic size effect constant for the number of elements result in an equivalent condition. The results are summarized in figure 2.1

An important quantity in terms of characterizing high-entropy alloys is the total number of electrons VEC. The valence electron concentration of

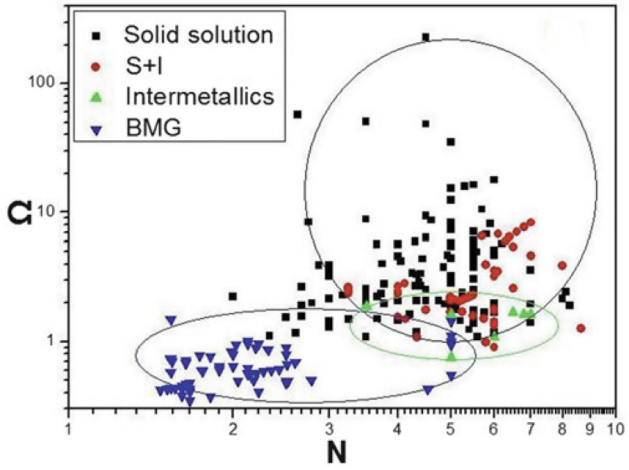

(a) HEA formation based on Ω and δ

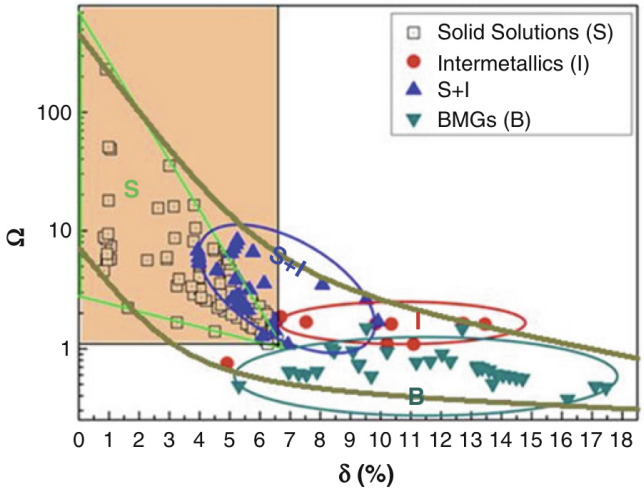

(b) HEA formation based on Ω and N

Figure 2.1: Formation of HEA based on δ and N. Figures adopted from [15]

a material is strongly related to the crystal structure of the material. For example, Co_3V, originally a hexagonal structure can be transformed into a tetragonal or cubic structure by either increasing the VEC from alloying with Ni, or reduction with Fe respectfully. Derived from the work of Guo et al. on the phase stability of a $Al_xCrCuFeNi_2$ HEA, the VEC can be directly related to the crystal structure of high-entropy alloys. A lower VEC stabilize the BCC phase, while higher values stabilize FCC. In between is a mixture of the two. Specifically values greater than 8.0 stabilize FCC, and values bellow 6.87 favor BCC. However, these boundaries is not rigid when including elements outside of transition metals, exceptions has also been found for high-entropy alloys containing Mn. All though a heavy majority of reported high-entropy alloys that form solid solutions have been found to adopt simple cubic structures such as FCC and BCC. Recent studies have observed HEA's in orthorombic structures like $Ti_{35}Zr_{27.5}Hf_{27.5}Ta_5Nb_5$ and hcp structures, for example $CoFeNiTi$.

2.2 Core effects and properties

Next, we will summarize the discussion above into four core effects of high entropy alloys coupled with the unique properties observed in HEAs. The first of these is called the "high-entropy effect", as explained in the previous section the configurational entropy of HEAs is much greater than in traditional solids or even binary alloys, this quantity is central to stabilize the disordered phase ahead of intermetalic or strongly ordered structures. Thus this effect can result in enhanced strength and ductility. From considerations of Gibbs free energy (Eq. 1), we see that this effect is most prominent at elevated temperatures.

The second effect is the "severe lattice distortion effect" that arises from the fact that every element in a high-entropy structure is surrounded by non-homogeneous elements, thus leading to severe lattice strain and stress. The overall lattice distortion is additionally attributed to the differences in atomic size, bonding energies and crystal structure tendencies between the components. Therefore the total lattice distortion observed in HEA's are significantly greater than that of conventional alloys. This effect mostly affect the strength and conductivity of the material, such that a higher degree of distortion yields greater strength and greatly reduces the electronic and thermal conductivity due to increased electron and phonon scattering. An upside to this is that the scattering and following properties become less temperature dependent given that it originates from the lattice rather than thermal vibrations.

The two remaining effects, "sluggish diffusion" and "cocktail effect" can be summarized swiftly. The first is a direct consequence of the multi-component layout of high-entropy alloys that result in slowed diffusion and phase transformation because of the number of different elements that is demanded in the process. The most notable product from this effect is an increased creep resistance. Lastly we have the cocktail effect, which is identical to the smoothie analogy mentioned previously, in that the

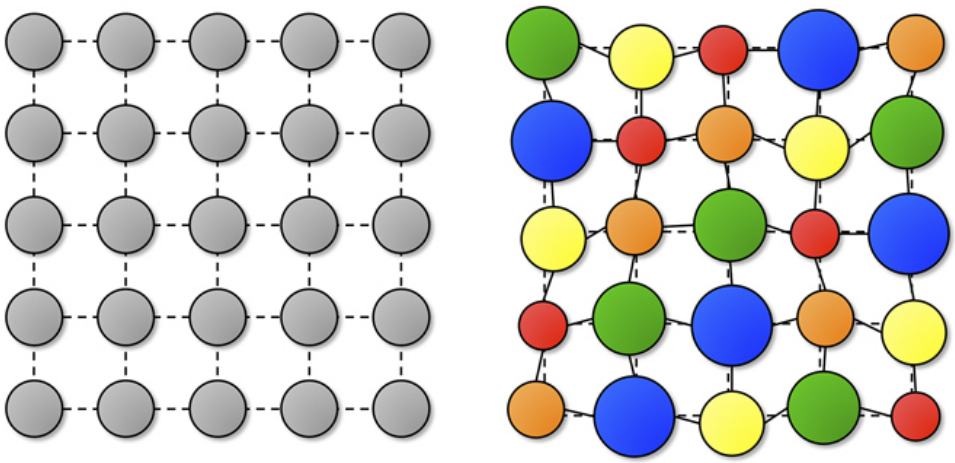

Figure 2.2: A schematic illustration of lattice distortion in high-entropy alloys. Figure from [3]

resultant characteristics is a combination of both the elements and their interaction. This is possible the most promising concept behind high-entropy alloys, which fuels researchers with ambition to discover highly optimized materials by meticulously combining and predicting properties from different elements. Examples of this can be the refractory HEA's developed by "Air Force Research Laboratory" severely exceeding the melting points and strength of previous Ni or Co-based superalloys by alloying specifically refractory elements such as Mo. Nb and W. Another example is the research conducted by Zhang et al. on the high-entropy system FeCoNi($AlSi_{0-0.8}$ in the intent of unveiling the optimal combination of magnetic, electric and mechanical properties, resulting in an excellent soft magnet.

In the discussion above, we have covered the four core effects that make up high-entropy alloys and their relation to the mechanical and functional properties. Of the core effects, especially the lattice distortion and cocktail effect relate to the functional properties. Next we will include some examples from recent studies on the functional properties of HEAs.

The H-x alloy, referring to the system $Al_xCoCrFeNi$ with $0 \leq x \leq 2$ have been subject to extensive investigation of functional properties. The electrical resistivity was higher than that of conventional alloys, and further decreased with increasing amounts of Al, noteworthy was also low carrier mobility. Similar findings have also been made for the high-entropy alloy $FeCoNi(AlSi)_x$.

Chapter 3

Modeling of random alloys

The structure of high-entropy alloys in which the alloying elements occupy lattice sites by a random probability pose a problem on the numerical methods used for modeling. DFT in particular rely heavily on the periodicity in crystalline solids, as we will discover later. In a brute force approach, this could be solved by randomly distribute the solute and solvent atoms over the lattice sites of a large supercell and average the energy and related properties of a great number of such supercells with varying distributions. Obviously this approach is rather efficient or even doable considering the computational demand. Thankfully today there exists a number of possible methods to more efficiently study such structures. Examples are the virtual crystal approximation (VCA), Coherent Potential approximation (CPA), special quasi-random structure (SQS), and hybrid monte-carlo/molecular dynamics. (MC/MD). A brief review of the different models is given in for example [6]. In this project we will employ the SQS method, due to both it's easy to use implementation and interpretation in VASP compared to the other options, and other benefits that will become clear after the following sections.

3.1 The Special Quasi-random Structure model

In the original paper on SQS published in 1990 [11], it was proposed a selective occupation strategy to design special periodic quasi-random structures that exceeded previous methods in both accuracy and cost. The key concept was to create a periodic unit cell of the various components in a finite N lattice site single configuration such that the structure most closely resemble the configuration average of an infinite perfect random alloy. In an attempt to work withing the 50 lattice sites boundary of ab initio methods at that time. The working theory was that if one can resemble an infinite perfect random alloy by a periodic finite N cell, also the electronic properties would be similar between the two. The solution to this model was that for each N, ie lattice site, to minimize the difference of structural correlation function between the approximated cell and the perfect random alloy. There are obviously errors involved with approximating a random alloy by a periodic cell, but by the hierarchical relation to the properties of

the material, interactions between distant sites only offer a negligible small contribution to the total energy of the system. Thus the aim of the SQS method is focused around optimizing the correlations within the first few shells of a given site. To follow is a review of the mathematical description of special quasi-random structures.

3.1.1 Mathematical description

We begin this section by giving a brief review of topics such as cluster expansions, statistics and superposition of periodic structures. A broader description of these topics can be found in the original article, or elsewhere in the literature. On a side note regarding the following mathematical derivation, the original concept was devolved in mind of an random binary alloy, but the theory have late successfully been extended to multi-component alloys and other special cases.

The different possible atomic arrangements are denoted as "configurations" σ. The various physical properties of a given configuration is $E(\sigma)$, and $< E >$ is the ensemble average over all configurations σ. In practice, this quantity is unfeasible in terms of computational cost, seeing as the average require calculations and relaxations of all possible configurations, for a binary alloy this is 2^N for a fixed N number of lattice sites. A solution to this is to use the theory of cluster expansions and discretize each configuration into "figures" f. A figure in the lattice is defined in terms of the number of atoms it include k, distance in terms of neighbors m, and position in the lattice l. Further we assign spin values for each lattice site i in the figure to denote which element it holds (+1,-1 for a binary alloy). By defining the spin product of spin variables in a figure at lattice position l as $\Pi_f(l, \sigma)$, we can write the average of all locations in the lattice of a given figure f as

$$\mathbf{\Pi}_f(\sigma) = \frac{1}{ND_f} \sum_l \Pi_f(l, \sigma) \tag{3.1}$$

where D_f is the number of equivalent figures f per site. The brilliance of this notation is that we now can express the physical property $E(\sigma)$ in terms of the individual contributions ϵ_f of a figure f.

$$E(\sigma) = \sum_{f,l} \Pi_f(l, \sigma) \epsilon_f(l) \tag{3.2}$$

The quantity ϵ_f is called the "effective cluster property" and is defined as (for a random binary alloy $A_{1-x}B_x$)

$$\epsilon_f(l) = 2^{-N} \sum_{\sigma}^{2^N} \Pi_f(l, \sigma) E(\sigma) \tag{3.3}$$

Inserting the equation for $\mathbf{\Pi}_f$ into that of $E(\sigma)$ we can describe the the previous cluster expansion of $E(\sigma)$ as

$$E = N \sum_f D_f < \mathbf{\Pi_f} > \epsilon_f \tag{3.4}$$

And obtain a simplified expression for $< E(\sigma >)$ in eq 1? Thus we have successfully managed to reduce the expensive task of sampling all $E(\sigma)$ into calculating the effective cluster properties and summing over all types of figures. Remembering that $E(\sigma)$ can relate to many physical properties, the most common and applied case is that $E(\sigma)$ is the total energy, while ϵ_f is many body interaction energies. The cluster expansion above converge rather quickly with increasing number of figures, an effective method is thus to select a set of configurations to evaluate the effective cluster properties. Don't know how to write this, but the next step is to select a finite largest figure denoted F, and "specialize" the cluster expansion to a set of N_s periodic structures σ =s to obtain the two expressions for $E(s)$ and ϵ_f using matrix inversion to obtain the result for ϵ_f

$$E(s) = N \sum_{f}^{F} D_f \mathbf{\Pi}_f(s) \epsilon_f \tag{3.5}$$

$$\epsilon_f = \frac{1}{ND} \sum_{s}^{N_s} [\mathbf{\Pi}_f(s)] - 1E(s) \tag{3.6}$$

Assuming now that the sum of figures F and N_s periodic structures are well converged, $E(\sigma)$ can be rewritten as a superposition of $E(s)$

$$E(\sigma) = \sum_{s}^{N_s} \xi_s(\sigma) E(s) \tag{3.7}$$

$$\xi_s(\sigma) = \sum_{f}^{F} [\mathbf{\Pi}_f(s)]^{-1} \mathbf{\Pi}_f(\sigma) \tag{3.8}$$

where ξ is the weights. Thus we have effectively reduced the problem to a convergence problem of the number of figures F and structures N_s. This can be easily solved given that we are dealing with periodic crystal structures s that can employ the general applications of ordered structures from ab initio methods, and increasing F until the truncation error falls bellow a desired threshold. However, this approach requires that the variance of the observable property is much lower than the sample mean, otherwise one would have to employ a much bigger sample size to reach statistical convergence. Don't how to write this part nicely, but: Because of the different relationship between various physical properties and the correlation functions, one observe different convergence depending on the meaning of E. The idea behind SQS was therefore to design single special structures with correlation functions $\mathbf{\Pi}_f(s)$ that most accurately match those of the ensemble average of a random alloy $< \mathbf{\Pi}_f >_R$.

The correlation functions of an perfect random infinite alloy, denoted as R is defined bellow

$$\mathbf{\Pi}_{k,m}(R) =< \mathbf{\Pi}_{k,m} >_R = (2x-1)^l \tag{3.9}$$

with k, m defined as before and x being the composition ratio of the alloy. In the case of an eqvimolar alloy ($x = \frac{1}{2}$), the functions equal 0 for all k

except $< \mathbf{\Pi}_{0,1} >_R = 1$. If we now randomly assign either atom A or B to every lattice site, for a sufficiently large value of N, the goal is then to create a single configuration that best match the random alloy. Keeping with the $x = \frac{1}{2}$ case, the problem is now that even though the average correlation functions of a large set of these structures approaches zero, like for the random alloy. The variance of the average is nonzero meaning that a selected structure of the sample is prone to contain errors. The extent of these errors can be evaluated from the standard deviations

$$\nu_{k,m}(N) = | < \mathbf{\Pi}^2_{k,m} > |^{\frac{1}{2}} = (D_{k,m}N)^{-\frac{1}{2}} \tag{3.10}$$

Given the computational aspects, it's obvious that economical structures with small N are prone to large errors. In fact, in some cases these errors can result in correlation functions centering around 1, as opposed to 0 for a perfect random alloy.

I don't know how to write the prelude to this part! (see section IIIA in [11]). The degree to which a structure s fails to reproduce the property E of the ensemble-averaged property of the random alloy can be described by a hierarchy of figures, see eq .. bellow

$$< E > -E(s) = \sum_{k,m}{}' D_{k,m}[(2x-1)^k - \mathbf{\Pi}_{k,m}(s)]\epsilon_{k,m} \tag{3.11}$$

, the prime is meant symbolize the absence of the value $0, 1$ for k, m. The contribution from the figure property ϵ reduces for larger figures. In general, for disordered systems, the physical property "E" at a given point R falls of exponentially as $|R - R'|/L$, where L is a characteristic length scale relating to the specific property. Using this, the approach of SQS is to specify a set of correlation functions that hierarchically mimic the correlation functions of the random alloy. Meaning that it prioritize the nearest neighbor interactions. With the set of functions decided on, the objective it finally to locate the structures that correspond to the selected structures.

With this approach, [11] managed by mimicking the correlation functions exact for the first two shells, to reduce the computational measures of an accurate models. In this exact study they matched the results of an $N \to \infty$ by an $N = 8$ SQS. In the final section of this chapter, we will take a look at the recent advances in the SQS method and application to high-entropy alloys.

3.1.2 Applications to high-entropy alloys

The success of the SQS method is in large part related to to the fact that we can create simple periodic structures, this allows for the use of standard DFT methods to calculate with ease properties such as the total energy, charge density and electronic band structure [2], [9]. However, some certain obstacles arise when trying to apply the SQS model to high-entropy alloys. An exhaustive analysis discussing several of these factors

and comparing to alternative methods were performed in 2016 by M.C Gao et al. [1] in the framework of DFT and VASP.

The first initial concern is the size of the supercell. This parameter needs to be balanced between accuracy and cost. A larger SQS cell consisting of a greater number of atoms better encapsulate the disordered structure of HEAs, but both the generation and simulation of such large SQSs come at an increased computational demand. M.C Gao discovered a significant sensitivity between the registered stability and predicted crystal structure of CoCrFeNi and CoCrFeMnNi HEAs and varying SQSs sizes. Experimentally both of these is found stable in the FCC structure. By calculating the enthalpy of formation, he found that SQSs under 64 atoms wrongly predicted the HCP structure as the most stable, while larger SQS correctly agreed on the FCC structure. Additionally, the probability distribution functions (PDFs) of the respective SQSs display a dependence to the SQS size. For example in 3 SQSs of size 20, 125 and 250 atoms each of FCC CrFeMnNi, the Cr-Mn is much better represented in the large SQS model as seen bellow in figure 4.1.

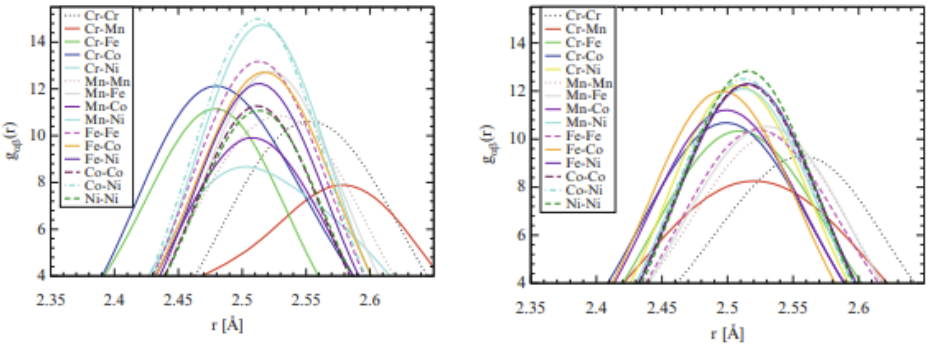

(a) 20 atom SQS

(b) 250 atom SQS

Figure 3.1: PDFs of (a) 20 and (b) 250 atom SQS models of CrFeMnNi [1]

It can also be noted that a similar dependence on the SQS size is apparent for the entropy and mechanical properties, however these topics are not relevant for this project and will thus not be elaborated further. Bellow we summarize the findings of M.C Gao et al between the SQS model and the crystal potential approximation and hybrid monte-carlo/molecular dynamics applied to high-entropy alloys. The comparison of SQS and MC/MD in terms of the calculated density of states can be seen in figure 3.2.

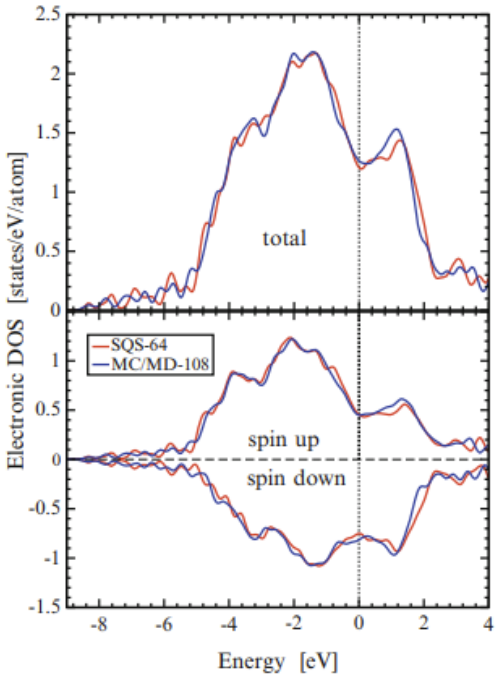

Figure 3.2: Density of states with SQS and MC/MD of FCC CoCrFeNi, figure from [1]

The density of states (DOS) of the MC/MD simulations were conducted on a larger 108 atom cell, compared to a 64 atom SQS. In despite of both the larger cell and much more complex calculations, the results of the SQS model measures up well. Furthermore, the SQS model produce a comparative outcome of the probability distribution functions (PDFs) to MC/MD as seen bellow.

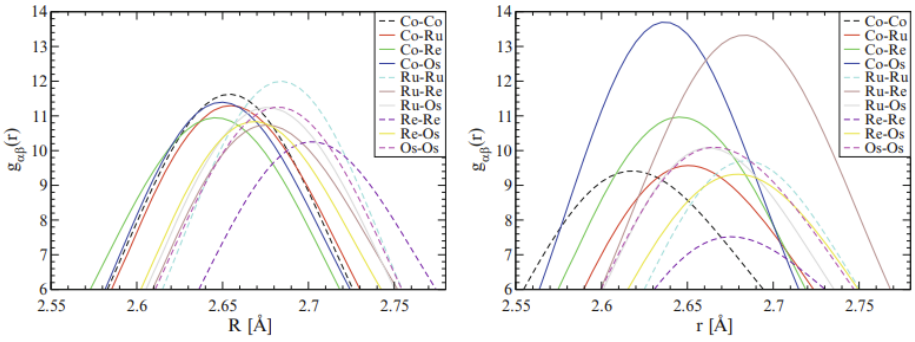

Figure 3.3: Probability distribution functions with SQS and MC/MD of HCP CoOsReRu [1]

The discrepancy in the PDFs are seen as more accurate from MC/MD calculations compared to experimental values. This is because SQS fail to include inter-atomic interaction and preference to the same extent as MC/MD. This is illustrated in figure 3.3 for the HCP CoOsreRu alloy, in which clear preference of Co-Os and Re-Ru pairs is apparent from MC/MD

simulations but not in the SQS model. Regardless, the results of SQS is very good considering the simplicity of the model and implementation. Compared to the CPA method, SQS is the less equipped method for dealing with specific cases such as $A_1/_3BCDE$ structures, and paramagnetic materials [1]

We have seen up until this point that the SQS method utilized an intelligent approach which allows for a simple implementation and calculations while providing results mostly on par to other more intricate and complex solutions to model disordered structures. However one particular factor concerning SQS that does not apply for CPA and MC/MD, is that within the SQS model one material can obtain in a number of distinct configurations. For example a quaternary and quinary alloy make for 24 and 124 unique configurations respectively, resulting in an uncertainty of the energy regarding the different permutations. This effect is most prominent in anisotropic lattices such as HCP and alloys with chemically dissimilar constituents, and particularly in small SQS cells [1].

Despite of it's flaws, especially in recent years SQS have emerged as a viable and trusted method of modeling disordered structures such as HEA. This is down to both the increasingly available computational power and improvements to the SQS method. The latter particularly saw a boost in 2013 with the introduction of the MC-SQS method [7], short for Monte-Carlo Special Quasirandom Structures. Contrary to the original SQS method that seek to minimize the difference between the correlation functions of the approximated cell and the true random alloy, this method employ monte-carlo simulations to perfectly match a maximum number of correlation functions. Furthermore emphasizes an efficient and fast implementation in addition to an exhaustive unbiased search of possible atomic configurations. Following, this is the preferred and most widely used method of choice in today's research, specific details on the method can be found in [7]. **How much detail do I need to include here, should I do a full explanation of the method or does this suffice?** This has resulted in an increased number of studies utilizing SQSs to investigate high-entropy alloys [8], [10], [4], and [5].

Part II

Methodology and Implementation

Part III

Results and Discussion

Part IV

Conclusion

Write conclusion here

Bibliography

[1] Michael C. Gao et al. 'Applications of Special Quasi-random Structures to High-Entropy Alloys'. In: *High-Entropy Alloys: Fundamentals and Applications*. Ed. by Michael C. Gao et al. Cham: Springer International Publishing, 2016, pp. 333–368. ISBN: 978-3-319-27013-5. DOI: 10.1007/978-3-319-27013-5_10. URL: https://doi.org/10.1007/978-3-319-27013-5_10.

[2] Z. W. Lu, S.-H. Wei and Alex Zunger. 'Electronic structure of ordered and disordered Cu_3 Au and Cu_3 Pd'. In: *Phys. Rev. B* 45 (18 May 1992), pp. 10314–10330. DOI: 10.1103/PhysRevB.45.10314. URL: https://link.aps.org/doi/10.1103/PhysRevB.45.10314.

[3] Lewis Robert Owen and Nicholas Gwilym Jones. 'Lattice distortions in high-entropy alloys'. In: *Journal of Materials Research* 33.19 (2018), pp. 2954–2969. DOI: 10.1557/jmr.2018.322.

[4] Muhammad Rashid et al. 'Ab-initio study of fundamental properties of ternary ZnO1-xSx alloys by using special quasi-random structures'. In: *Computational Materials Science* 91 (2014), pp. 285–291. ISSN: 0927-0256. DOI: https://doi.org/10.1016/j.commatsci.2014.04.032. URL: https://www.sciencedirect.com/science/article/pii/S0927025614002742.

[5] V. Sorkin et al. 'First-principles-based high-throughput computation for high entropy alloys with short range order'. In: *Journal of Alloys and Compounds* 882 (2021), p. 160776. ISSN: 0925-8388. DOI: https://doi.org/10.1016/j.jallcom.2021.160776. URL: https://www.sciencedirect.com/science/article/pii/S092583882102185X.

[6] Fuyang Tian. 'A Review of Solid-Solution Models of High-Entropy Alloys Based on Ab Initio Calculations'. In: *Frontiers in Materials* 4 (2017). ISSN: 2296-8016. DOI: 10.3389/fmats.2017.00036. URL: https://www.frontiersin.org/article/10.3389/fmats.2017.00036.

[7] A. van de Walle et al. 'Efficient stochastic generation of special quasirandom structures'. In: *Calphad* 42 (2013), pp. 13–18. ISSN: 0364-5916. DOI: https://doi.org/10.1016/j.calphad.2013.06.006. URL: https://www.sciencedirect.com/science/article/pii/S0364591613000540.

[8] Shen Wang et al. 'Comparison of two calculation models for high entropy alloys: Virtual crystal approximation and special quasi-random structure'. In: *Materials Letters* 282 (2021), p. 128754. ISSN: 0167-577X. DOI: https://doi.org/10.1016/j.matlet.2020.128754. URL: https://www.sciencedirect.com/science/article/pii/S0167577X20314610.

[9] Su-Huai Wei and Alex Zunger. 'Band offsets and optical bowings of chalcopyrites and Zn-based II-VI alloys'. In: *Journal of Applied Physics* 78.6 (1995), pp. 3846–3856. DOI: 10.1063/1.359901. eprint: https://doi.org/10.1063/1.359901. URL: https://doi.org/10.1063/1.359901.

[10] Peng Wei et al. 'Understanding magnetic behaviors of FeCoNiSi0.2M0.2 (M=Cr, Mn) high entropy alloys via first-principle calculation'. In: *Journal of Magnetism and Magnetic Materials* 519 (2021), p. 167432. ISSN: 0304-8853. DOI: https://doi.org/10.1016/j.jmmm.2020.167432. URL: https://www.sciencedirect.com/science/article/pii/S0304885320323994.

[11] S.-H. Wei et al. 'Electronic properties of random alloys: Special quasirandom structures'. In: *Phys. Rev. B* 42 (15 Nov. 1990), pp. 9622–9649. DOI: 10.1103/PhysRevB.42.9622. URL: https://link.aps.org/doi/10.1103/PhysRevB.42.9622.

[12] Jien-Wei Yeh. 'Overview of High-Entropy Alloys'. In: *High-Entropy Alloys: Fundamentals and Applications*. Ed. by Michael C. Gao et al. Cham: Springer International Publishing, 2016, pp. 1–19. ISBN: 978-3-319-27013-5. DOI: 10.1007/978-3-319-27013-5_1. URL: https://doi.org/10.1007/978-3-319-27013-5_1.

[13] Jien-Wei Yeh. 'Physical Metallurgy'. In: *High-Entropy Alloys: Fundamentals and Applications*. Ed. by Michael C. Gao et al. Cham: Springer International Publishing, 2016, pp. 51–113. ISBN: 978-3-319-27013-5. DOI: 10.1007/978-3-319-27013-5_3. URL: https://doi.org/10.1007/978-3-319-27013-5_3.

[14] Jien-Wei Yeh et al. 'Functional Properties'. In: *High-Entropy Alloys: Fundamentals and Applications*. Ed. by Michael C. Gao et al. Cham: Springer International Publishing, 2016, pp. 237–265. ISBN: 978-3-319-27013-5. DOI: 10.1007/978-3-319-27013-5_7. URL: https://doi.org/10.1007/978-3-319-27013-5_7.

[15] Yong Zhang et al. 'Phase Formation Rules'. In: *High-Entropy Alloys: Fundamentals and Applications*. Ed. by Michael C. Gao et al. Cham: Springer International Publishing, 2016, pp. 21–49. ISBN: 978-3-319-27013-5. DOI: 10.1007/978-3-319-27013-5_2. URL: https://doi.org/10.1007/978-3-319-27013-5_2.